Exploring high strength metallic materials: a lesson from pearlitic steel wire

Zhang, X.

Published in:
I O P Conference Series: Materials Science and Engineering

Link to article, DOI:
10.1088/1757-899x/580/1/012058

Publication date:
2019

Document Version
Publisher's PDF, also known as Version of record

Exploring high strength metallic materials: a lesson from pearlitic steel wire

IOP Conf. Series: Materials Science and Engineering **580** (2019) 012058 doi:10.1088/1757-899X/580/1/012058

Exploring high strength metallic materials: a lesson from pearlitic steel wire

X Zhang

Section of Manufacturing Engineering, Department of Mechanical Engineering, Technical University of Denmark, 2800 Kgs, Lyngby, Denmark

Email: xzha@mek.dtu.dk

Abstract. In human history, the development of stronger materials through the ages is reflected with names of eras illustrating our progress. Besides phase transformations, plastic deformation is one of the major methods to produce products with reliable and predictable mechanical properties such as strength. Pearlitic steel wire, the strongest mass-produced steel, shows an excellent combination of formability and strength. The present overview summarizes the investigation of cold-drawn pearlitic steel wires over the last 150 years, covering the pearlite phase transformation, chemical composition design for wires with high strength, microstructure evolution during wire drawing, strengthening mechanisms and structure-strength relationships. By focusing on the structure, challenges and future strategy are outlined to further improve the strength and performance of pearlitic steel wire, where these routes may also applicable to other metals.

1. Introduction

In the history of mankind and civilization, the drive to develop stronger materials through the ages is evidence by with names of eras illustrating our progress [1]. Metals are the major structural material in our society due to their unique properties such as high reliability with predicable strength, excellent fracture toughness compared with other materials (engineering polymetric composites and ceramics) and recyclability for the large scale application. These properties will also make them irreplaceable in the future [2]. However, there exist limitations from case to case in the properties of metals as they are currently used, with a major one being the low specific strength.

Very high strengths, up to 13 GPa have been observed in the tensile and compression testing of microscale and nanocale single crystal metals. These single crystal metals are made by crystal growth or other chemical processes and they are normally quite small (less than 10 micrometer). Moreover, many of these single crystal metals show catastrophic failure without any observable amount of plastic deformation [3]. As a result, such small single crystal metals are rarely used for structural applications.

Metals can be strengthened through controlled introduction of internal defects and boundaries that obstruct dislocation motion. Most of the structural metals used in the industry and our daily lives are polycrystalline and an effective way for improvement of strength is deformation at low temperature ($T \leq 0.35\ T_M$), resulting in an increase of strength by up to two orders of magnitude (where T_M is the melting temperature) due to the increase of internal defects and boundaries [4]. Accompanying the strength increase, the ductility is reduced and the grain size is refined. Very strong steels can also be

produced by plastic deformation to very high strain but drawbacks are the large working force required and the poor formability of the final deformed product [5]. These steels owe their strength to a very fine scale microstructure containing a large concentration of defects in the form of dislocations and boundaries. Strong steels, such as bainitic and martensitic steels, can also be produced by phase transformation [6, 7]. One objective of both research and development has therefore been to optimize the different processes and the desired structural refinement.

Nowadays, the maximum flow stress in metals applied in industry (E/100 - E/50) is far from the ideal strength, except for the case of a few metals. Cold-drawn pearlitic wire, with a microstructure resulting from a combination of phase transformation and plastic deformation, widely applied for uses including cables for suspension bridges, steel cords for automobile tires and springs, is one of these. Pearlitic wire is in fact the strongest mass-produced metal, with a maximum strength of 4.8 ~ 5.7 GPa (E/44 ~ E/37), for the grain size around 11 nm [8, 9], and the laboratory record strength around 6.8 GPa (E/31) for a grain size of 10 nm [10]. This high-strength pearlitic wire also excellent properties, with the strength-to-weight comparable to ceramics and carbon fibers but much better fracture toughness (a measure of the energy required for propagating cracks) [11]. These outstanding properties of the nanostructured material guarantee its application in large-scale structures such as the Great Belt Bridge.

The present overview summarizes investigations of cold-drawn pearlitic steel wires in the last several decades, covering topics of of pearlite phase transformation and wire chemical composition design for high strength, microstructure evolution during wire drawing, strengthening mechanisms and structure-strength relationships. Challenges and future strategy are outlined and an outlook to further improve the strength and performance of pearlitic steel wire and other metals is given.

2. Pearlite Phase Transformation and Wire Chemical Composition Design for High Strength

Pearlite is the product of austenite decomposition by a eutectoid reaction. The pearlite phase transformation provides an excellent example of the historical development of phase transformations, where the ‘hardening problem’ in steel was pursued in the 1880–1925 period using metallography, thermal analysis, and the Gibbs phase rule. Breakthroughs were afforded by X-ray diffraction and other techniques such as transmission electron microscopy regarding metal structure, phase structure and phase transformations in the period of 1925–1970 [12], illustrating the importance of interaction between experimental observations and the development of quantitative models. The pioneering work of Davenport and Bain [13] provided a basis for the development of time-temperature-transformation (TTT) diagrams and the ability to quantify and rationalize the role of alloying elements in terms of hardenability and their influence on structure-property relationships in steels [14]. This was followed by a quantitative description of nucleation and growth rates and interlamellar spacing via a detailed microstructural approach [15], a detailed discussion of analytical and experimental aspects of nucleation and growth kinetics [16], a description of 3D structure from 2D observations [17] and the theory of diffusional growth [18]. The importance of both volume diffusion [19, 20] and diffusion at the advancing interface was first recognized in the 1970s and different models have since been proposed [21, 22] as the rate of motion of the interface in solid state reactions can be controlled by diffusion and thus a large undercooling can occur. Meanwhile, the crystallographic aspects of the pearlite phase transformation including the ferrite-austenite, ferrite-cementite and cementite-austenite orientation relationships have were actively investigated from the 1950s to 1990s [17, 23-27].

Since carbon is the most effective element to harden the steel, hypereutectoid steel with carbon content higher than 0.8 wt% has been investigated for development of high strength steel wires in the industry from the very beginning, and later the combined effect of patenting conditions, cooling rate, chemical composition on pearlite lamellar spacing has been widely investigated [9]. To obtain a high drawability and a high work hardening rate, an appropriate cooling rate corresponding to carbon content should be secured to prevent precipitation of thick proeutectoid cementite. The thickness of cementite lamellae as well as the interlamellar spacing decreases with the increase of carbon content in the practical patenting temperature range. Finally, small-diameter (down to several tens of

micrometers) high-strength steel wires with the present strength record have been manufactured on a production basis with a chemical composition typically around 0.96C-0.2Si-0.3Mn-0.2Cr (wt-%) [10].

3. Microstructure Evolution during Wire Drawing

The pearlitic lamellar structure, as shown in figure 1, consists of alternating ferrite and cementite layers as a result of the decomposition of eutectoid austenite, where pearlite colonies with different oriented lamellae nucleate from prior austenite boundaries and form in one austenite grain [14, 28-30]. The first images of pearlite were shown by Sorby at the British Association meeting in September 1864 [31], and drawn pearlitic wires date back to 1886 when wires with a carbon content of 0.828 wt% and a strength not less than 1.65 GPa were produced for military applications [32]. The wire drawing up to medium strains reorients the initial random lamellar directions of different pearlite colonies to the drawing direction [33-36] in the longitudinal direction, while curling of the lamellar structure takes place in the cross-section, as is characteristic [35, 37] for drawing of a bcc metal [4, 38, 39]. Further drawing to large strains continuously thins down the ferrite lamellae with increasing dislocation densities [8, 40] and leads eventually to decomposition of cementite lamellae [8, 10, 41-46]. Detailed microstructural characterization in the last 50 years by transmission electron microscopy (TEM) [40, 47-49], high resolution electron microscopy (HREM) [8] and three dimensional atom probe (3DAP) [45, 46, 50] has quantified the systematic evolution of microstructural parameters with the drawing strain, such as the interlamellar spacing (ILS), the thickness of ferrite (F) and cementite lamellae (C), the dislocation density in the ferrite lamellae and the carbon content in the ferrite lamellae. The major dislocation structure in the ferrite lamellae transforms from threading dislocations and tangles at low and medium strains, to dislocation cells at high strains, see figure 2. The final lamellar size depends on both the drawing strain and the chemical composition, which influences the dynamic recovery during drawing, but can be down to 10 nm in highly drawn wires (see figure 2b) [8, 9].

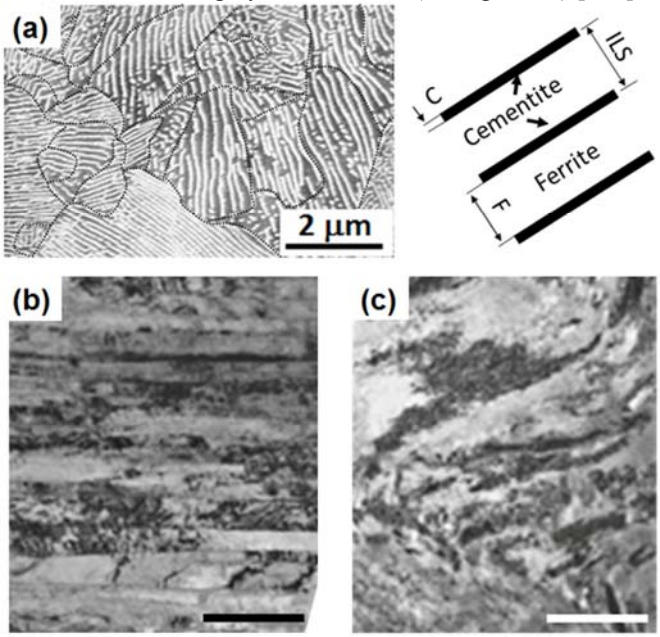

Figure 1. Scanning (a) and transmission (b and c) electron micrographs showing the alternating ferrite and cementite lamellae in the original as-patented state (a), the refined parallel lamellar structure in the longitudinal section (b) and the curling structure in the cross section (c) at a drawing strain of 3.7. The dashed lines in (a) show the pearlite colony boundaries. [30]

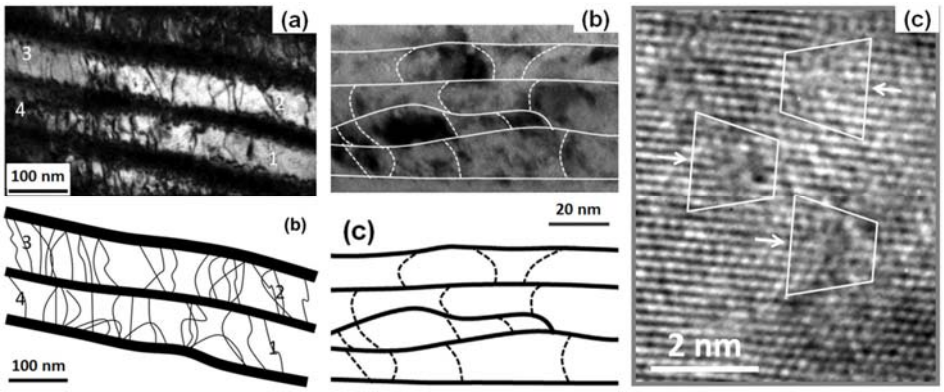

Figure 2. Transmission electron micrographs and sketches showing two major dislocation structures in the deformed ferrite lamellae: threading dislocations (thin lines) at a drawing strain of 0.7 (a), dislocation boundaries (dashed lines) (b) and atomic structure of a low angle dislocation boundary (c) at a drawing strain of 5.4. The thick black lines in the sketches represent cementite lamellae (a) or interfaces between neighboring ferrite lamellae (b). [8, 40]

Table 1. Microstructural parameters of a pearlitic wire containing 0.8 wt-% C in the drawing strain range from 0 to 5.4 [8, 40]

Strain	0	0.7	1.5	2.7	3.7	4.2	5.4
F (nm)	70	56	45	23	18	14	11
C (nm)	19	14	10	5	2	1.4	0.7
ρ (m^{-2})	8×10^{13}	7×10^{14}	2×10^{15}	9×10^{15}	2×10^{16}	3×10^{16}	5×10^{16}

4. Strengthening Mechanisms and Structure-Strength Relationship

Based on the recently elaborate quantification of the microstructural parameters [8, 40, 50], the previous one-parameter (ILS) structure-strength relationship proposed around 1970s [47, 49] has been extended to take into account the thickness of the ferrite (F) and cementite lamellae (C), the dislocation density in the ferrite lamellae, and the carbon content in the ferrite lamellae, as a results of a detailed analysis of the strengthening mechanisms (Table 1). The boundary strengthening is related to the ferrite lamellar thickness as the role of the cementite lamellae is estimated based on a Hall-Petch relation. The dislocation strengthening is related to the dislocation density in the ferrite lamellae through forest hardening proportional to its square root, and the solid solution hardening is related to carbon enrichment in the ferrite lamellae through the cementite decomposition, based on the interaction between dislocation configurations and carbon atoms in solution [8, 50].

Addition of contributions from the above three strengthening mechanisms plus the friction stress, gives a flow stress in good agreement with the experimental values ($\sigma_{0.2\%}$) up to the drawing strain around 2.7. At larger strains beyond 2.7, there exists a difference of around 10% between the experimental and calculated values (Table 2). The overestimation at large strains may have different reasons including: (i) regarding boundary strengthening, the deformation and decomposition of cementite lamellae may reduce the boundary resistance, leading to a reduced Hall-Petch coefficient, however, this reduction may be counteracted by carbon atom segregation to the interfaces between the ferrite lamellae and high angle boundaries/high density of dislocations at the interfaces; (ii) for the calculation of dislocation strengthening contribution using $\alpha MGb\sqrt{\rho}$, a choice of $\alpha = 0.24$, derived for tensile-tested samples with a smaller dislocation density by one to two orders [51], has been used. The value of α is actually proportional to $\ln(R/b)$ where R is the upper cut-off radius and can be taken as the average dislocation spacing ($\rho^{-0.5}$). This means that α may be smaller than 0.24, and a reduced contribution from dislocation strengthening may thus be expected; (iii) for the evaluation of solid solution hardening contributions, models for martensite have been applied [52, 53]. However, the deformation introduced distribution of dislocations and carbon atoms in the heavily drawn wires may

be different, which may introduce an overestimation of the flow stress. Additionally, dynamic recovery, which includes dislocation interactions and annihilation, has not been taken into account in the flow stress calculation.

Table 2. Experimental and calculated flow stress in the drawing strain range from 0 to 5.4 [8]

Strain	0	0.7	1.5	2.7	3.7	4.2	5.4
$\sigma_{exp,\ 0.2\%}$ (MPa)	880	1286	1614	2365	3395	3887	4510
σ_{cal} (MPa)	966	1230	1662	2370	3743	4251	5042
σ_{diff} (MPa)	86	−56	48	5	338 (10%)	364 (9%)	532 (12%)

5. Conclusions and Outlook

The present overview summarizes the investigations of cold-drawn pearlitic steel wires in the last 150 years with the aim to further improve the strength and performance of pearlitic steel wire and other metals.

- Based on the systematic and detailed characterization of drawn wires in the strain range from 0 to 2.7 with a lamellar scale above 20 nm, a good agreement has been found between the experimental flow stresses and calculated flow stresses, taking into account the traditional strengthening mechanisms.
- Challenges and a future research strategy can be: for the structural scale < 20 nm, new advanced microstructural and mechanical characterization techniques [54, 55] including in-situ TEM deformation technique [56] should be further developed. Moreover, the interaction between dislocations and solutes needs further detailed investigation to understand the structure-strength relationship, including the effects of dynamic recovery.

Based on the example of pearlitic steel wire, future development of high strength metallic materials and products, should combine the chemical composition design, phase transformation, dynamic processes and production processes, with the goal of achieving high strength while maintaining formability.

Acknowledgements

X Zhang acknowledge support from the European Research Council (ERC) under the the European Union Horizon 2020 research and innovation programme (grant agreement No 788567-M4D).

References

[1] National Research Council 1975 *Materials and man's needs: materials science and engineering -- volume I* Washington (DC): The National Academies Press
[2] Lu K 2010 *Science* **328** 319
[3] Brenner S S 1956 *J Appl Phys.* **27** 1484
[4] Gil Sevillano J 1980 *Progress in materials science* **25** 69
[5] Tsuji N and Maki T 2009 *Scripta Mater* **60** 1044
[6] Christian J W 2002 *The Theory of Transformations in Metals and Alloys* Pergamon
[7] Bhadeshia H K D H, 2010 *Proc R Soc A* **466** 3
[8] Zhang X, Hansen N, Godfrey A and Huang X 2016 *Acta Mater.* **114** 176
[9] Ochiai M, Nishida S, Ohba H and Kawata H 1993 Tetsu-to-Hagane **79** 1101
[10] Li Y, Raabe D, Herbig M, Choi P P, Goto S, Kostka A, Yarita H, Borchers C and Kirchheim R 2014 *Phy Rev Lett.* **113** 106104
[11] Hohenwarter A, Völker B, Kapp M W, Li Y, Goto S, Raabe D and Pippan R 2016 *Sci Rep.* **6** 33228
[12] Hackenberg R E 2012 *Phase transformations in steels Volume 1*, ed E Pereloma and D V Edmonds (Cambridge: Woodhead Publishing Limited) p 3
[13] Davenport E S and Bain E C 1930 *Trans AIME* **90** 117
[14] Embury D 2012 *Phase transformations in steels Volume 1*, ed E Pereloma and D V Edmonds (Cambridge: Woodhead Publishing Limited) p 276
[15] Mehl R F and Hagel W C 1956 *Progress in Metal Physics* **6** 74
[16] Cahn J W and Hagel W C 1962 *The Decomposition of Austenite by Diffusional Processes*, ed V

F Zackay and H I Aaronson (New York: Wiley) p 131
[17] Hillert M 1962 *The Decomposition of Austenite by Diffusional Processes*, ed V F Zackay and H I Aaronson (New York: Wiley) p 197
[18] Kirkaldy J S 1962 *The Decomposition of Austenite by Diffusional Processes*, ed V F Zackay and H I Aaronson (New York: Wiley) p 39
[19] Brown D and Ridley N 1969 *J Iron Steel Inst* **207** 1232
[20] Puls M and Kirkaldy J S 1972 *Metall Trans* **3** 2777
[21] Hashiguchi K and Kirkaldy J S 1984 *Scan J Metall* **13** 240
[22] Pandit A S and Bhadeshia H K B D 2011 *Proc R Soc A* **467** 508
[23] Bagaryatski Y A 1950 *Dokl Akad Nauk SSSR* **73** 1161
[24] Pitsch W 1962 *Acta Metall* **10** 79
[25] Lupton D F and Warrington D H 1972 *Acta Metall* **20** 1325
[26] Dippenaar R J and Honeycombe R W K 1973 *Proc R Soc A* **333** 455
[27] Zhou D S and Shiflet G J 1992 Metall Trans A 23 1259
[28] Zhang X, Hansen N, Godfrey A and Huang X 2012 *33rd Risø international symposium on materials science: Nanometals – status and perspectives* (Risø, Denmark) p 407
[29] Zhang X, Hansen N, Godfrey A and Huang X 2014 *35th Risø International Symposium on Materials Science: New Frontiers of Nanometals* (Risø, Denmark) p 153
[30] Zhang X, Hansen N, Godfrey A and Huang X 2018 *Mater Sci Technol* **34** 794
[31] Sorby H C 1864 *Report of the 34th meeting of British Assn Adv Science* Part II
[32] Percy J 1886 *J Iron Steel Inst* **29** 62
[33] Zhang X, Godfrey A, Hansen N, Huang X, Liu W and Liu Q 2010 *Mater. Charac* **61** 65
[34] Zhang X, Godfrey A, Liu W and Liu Q 2010 *Acta Metall Sin* **46** 141
[35] Zhang X D, Godfrey A, Liu W and Liu Q 2011 *Mater. Sci. Techno* **27** 562
[36] Zhang X, Godfrey A, Hansen N and Huang X 2013 *Acta Mater* **61**, 4898
[37] Langford G 1977 *Metall Trans A* **8** 861
[38] Hosford W F 1964 *Trans Met Soc AIME* **230** 12
[39] Aernoudt E Van Houtte P and Leffers T 1993 *Plastic deformatio and fracture of materials* (Weinheim: VCH, Newyork; Basel; Cambridge) p 129
[40] Zhang X, Godfrey A, Huang X, Hansen N and Liu Q 2011 *Acta Mater* **59** 3422
[41] Hong M H, Reynolds W T, Tarui T and Hono K 1999 *Metall Mat Trans A* **30** 717
[42] Gavriljuk V G 2003 *Mater Sci Eng A* **345** 81
[43] Languillaume J, Kapelski G and Baudelet B 1997 *Acta Mater* **45** 1201
[44] Hono K, Ohnuma M, Murayama M, Nishida S, Yoshie A and Takahashi T 2001 *Scr Mater* **44** 977
[45] Takahashi J, Tarui T and Kawakami K. 2009 *Ultramicroscopy* **109** 193
[46] Sauvage X, Lefebvre W, Genevois C, Ohsaki S and Hono K 2009 *Scr Mater* **60** 1056
[47] Embury J D and Fisher R M 1966 *Acta Metall* **14** 147
[48] Zhang X, Godfrey A, Huang X, Hansen N, Liu W and Liu Q 2009 *30th Risø international symposium on materials science: nanostructured metals – fundamentals to applications* (Risø, Denmark) p 409
[49] Langford G 1970 *Metall Trans A* **1** 465
[50] Li Y J, Choi P, Borchers C, Westerkamp S, Goto S, Raabe D and Kirchheim R 2011 *Acta Mater* **59** 3965
[51] Hansen N and Huang X 1998 *Acta Mater* **46** 1827
[52] Krauss G 1999 *Mater Sci Eng A* **273-275** 40
[53] Winghell P G and Cohen M 1963 *Electron microscopy and strength of crystals* (Interscience Publishers: New York) p 995
[54] Zhang X, Bech J I and Hansen N 2015 *IOP Conf Ser Mater Sci Eng* **89** 012158
[55] Zhang X, Nielsen C V, Hansen N, Silva C M A and Martins P A F 2019 *Int. J. Plast.* **115** 93
[56] Zhang X, Godfrey A, Hansen N, Huang X, Liu W and Liu Q 2010 *Mater Charac* **61** 65